NANO LETTERS

2006
Vol. 6, No. 4
662−668

Determining the Size and Shape Dependence of Gold Nanoparticle Uptake into Mammalian Cells

B. Devika Chithrani,[†,‡] Arezou A. Ghazani,[†,‡] and Warren C. W. Chan*[,†,‡,§]

Institute of Biomaterials & Biomedical Engineering, University of Toronto, 4 Taddle Creek Road, Toronto, Ontario M5S 3G9, Canada, Terrence Donnelly Center for Cellular and Biomolecular Research, University of Toronto, 160 College Street, 4th Floor, Toronto, Ontario M5S 3E1, Canada, and Materials Science and Engineering, University of Toronto, 184 College Street, Toronto, Ontario M5S 3E4, Canada

Received December 4, 2005; Revised Manuscript Received February 14, 2006

ABSTRACT

We investigated the intracellular uptake of different sized and shaped colloidal gold nanoparticles. We showed that kinetics and saturation concentrations are highly dependent upon the physical dimensions of the nanoparticles (e.g., uptake half-life of 14, 50, and 74 nm nanoparticles is 2.10, 1.90, and 2.24 h, respectively). The findings from this study will have implications in the chemical design of nanostructures for biomedical applications (e.g., tuning intracellular delivery rates and amounts by nanoscale dimensions and engineering complex, multifunctional nanostructures for imaging and therapeutics).

The chemical design and synthesis of nanoparticles have fueled the growth of nanotechnology. The foundation of nanotechnology research is based on the size and shape of the structures, where distinct optical, electronic, or magnetic properties can be tuned during chemical synthesis. There is an enormous interest in exploiting nanoparticles in various biomedical applications since their size scale is similar to that of biological molecules (e.g., proteins, DNA) and structures (e.g., viruses and bacteria). Furthermore, useful properties can be incorporated into the design of the nanoparticles for manipulation or detection of biological structures and systems. Nanoparticles are currently used in imaging, [1−6] biosensing,[7−9] and gene and drug delivery.[10−12]

As the field continues to develop, quantitative and qualitative studies on the cellular uptake of nanoparticles, with respect to their size and shape, are required in order to advance nanotechnology for biomedical applications. This will be important for assessing nanoparticle toxicity (i.e., if nanoparticles do not enter cells, they are less prone to killing cells or altering cellular function), for advancing nanoparticles for imaging, drug delivery, and therapeutic applications (i.e., how to maximally accumulate nanoparticles in cells, tumors, and organs?), and for designing multifunctional nanoparticles (i.e., are there dimensional limits to designing nanoparticles that can target and kill diseased cells?). Detailed studies of uptake kinetics of nanoparticles by cells have not been well characterized and quantified as a function of their size and shape (i.e., trends have not been determined). Most studies have focused on liposomes [13−16] and polymer particles,[17,18] which are generally larger than 100 nm. Furthermore, metallic, semiconductor, and carbon-based nanoparticles can be synthesized with greater size and shape variabilities than liposome and polymer particles.

We selected gold nanoparticles as the model system for our studies; the rationale being that gold nanoparticles could be synthesized at a large size (1−100 nm diameter) and shape range (1:1 to 1:5 aspect ratio). Gold nanoparticles are also easy to characterize by the techniques of UV−vis spectrophotometry, inductively coupled plasma atomic emission spectroscopy (ICP-AES), and transmission electron microscopy (TEM). Furthermore, gold nanoparticles have recently been demonstrated in cell imaging,[19,20] targeted drug delivery,[21] and cancer diagnostics and therapeutic applications.[22−25] These studies appear to be representative of the initial applications of nanoparticles in biology and medicine. In this paper, we studied the effect of nanoparticle size, shape, concentration, and incubation time on their cellular uptake kinetics. In the first part of the paper, the effect of nanoparticle size, concentration, and incubation time on the cellular uptake is discussed using colloidal gold nanoparticles with sizes varying between 14 and 100 nm. The second part of the paper is focused on the effect of nanoparticle shape on cellular uptake.

* Corresponding author. E-mail: warren.chan@utoronto.ca.
† Institute of Biomaterials & Biomedical Engineering.
‡ Terrence Donnelly Center for Cellular and Biomolecular Research.
§ Materials Science and Engineering.

10.1021/nl052396o CCC: $33.50
Published on Web 03/01/2006

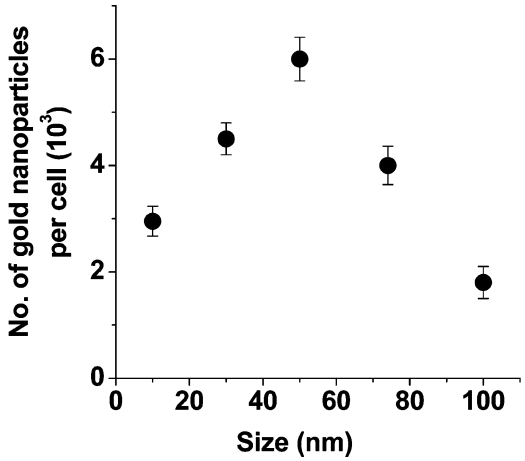

Figure 1. Dependence of cellular uptake of gold nanoparticles as a function of size.

Spherical and rod-shaped nanoparticles with diameters of 14, 30, 50, 74, and 100 nm and length by width of 40 × 14 nm and 74 × 14 nm, respectively, were prepared using standard solution techniques (see Supporting Information sections 1 and 2).[26−29] The spherical gold nanoparticles were free from aggregation (as determined by TEM, spectrophotometry, and gel electrophoresis) and had a size variation of ±10%. The surface of the spherical gold nanoparticles was not modified, and therefore, they were stabilized by citric acid ligands. Rod-shaped nanoparticles were synthesized using seed mediated growth as demonstrated by El-Sayed and Murphy and their co-workers.[28,29] After synthesis, the presence of rod-shaped, pyramid, and sphere-shaped nanoparticles was apparent in the TEM images. The majority of the nanoparticles were rod shaped (>75%) with a size variation of ±10%. The surface of the rod-shaped gold nanoparticles was modified by chemical exchange so that the cetyl trimethylammonium bromide (CTAB) was replaced by citric acid ligands. Fourier transform infrared (FTIR) spectroscopy showed the presence of citric acid on the surface of the nanoparticles; however, we cannot verify the complete removal of the rod-shaped gold nanoparticle's surface CTAB molecules due to the lack of available analytical techniques.

In these experiments, we incubated HeLa cells with gold nanoparticles with various sizes and shapes for 6 h in Dulbecco Minimum Essential Media (DMEM) plus 10% serum. After the allotted time, we detached the cells from the Petri dish surface using the enzyme trypsin, homogenized the cells, and measured the concentration of Au by the technique of ICP-AES. We used the following equations to convert the number of gold atoms to number of gold nanoparticles from the ICP-AES measurements. For a sphere of diameter *D*, the number of atoms (*U*) fitting into each volume of gold nanoparticles was determined. In this

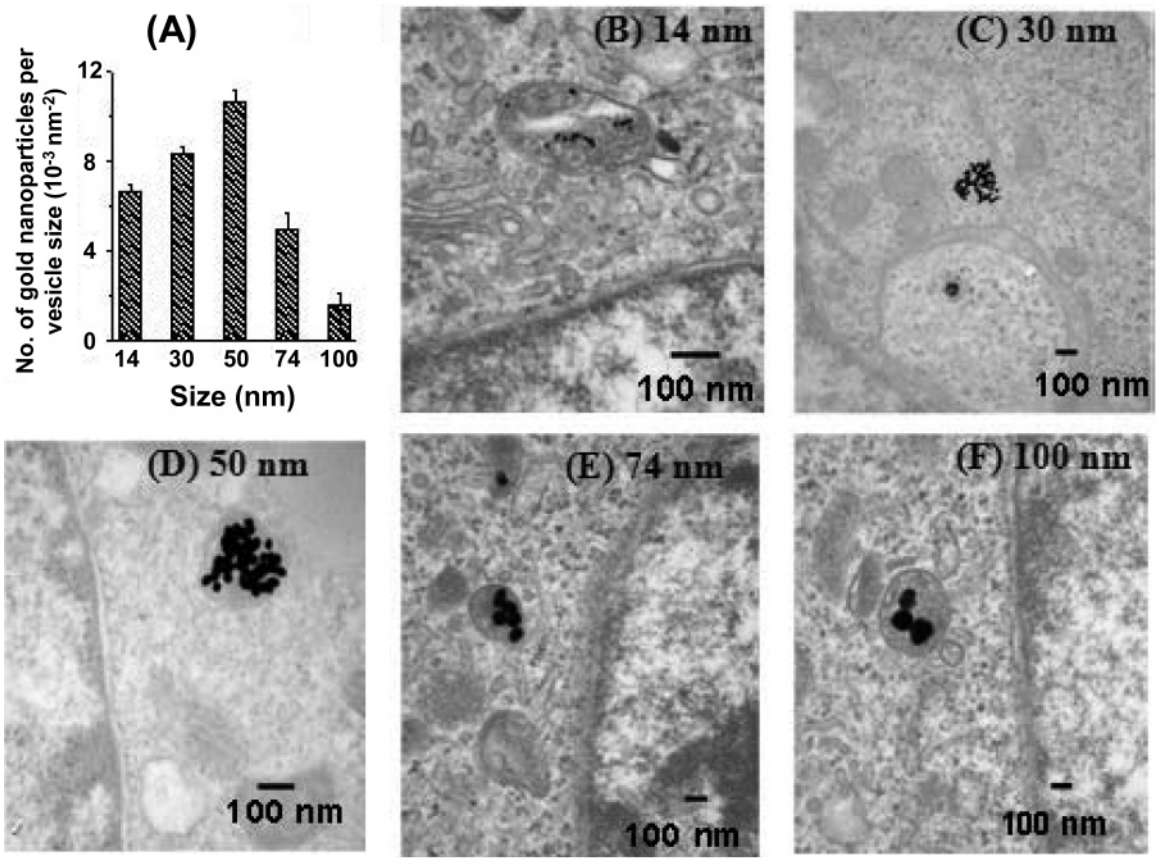

Figure 2. Transmission electron microscopy imaging and measurements of gold nanoparticles in cells. (A) The graph of number of gold nanoparticles per vesicle diameter vs nanoparticle size. (B−F) TEM images of gold nanoparticles with sizes 14, 30, 50, 74, and 100 nm trapped inside vesicles of a Hela cell, respectively. (TEM images were recorded at a voltage of 75 kV with a Hitachi H7000.)

calculation, a refers to the edge of a unit cell, which has a value of 4.0786 Å on the edge; there are four gold atoms per unit cell. M is the measured number of gold atoms from ICP-AES.

$$U = \frac{2}{3}\pi\left(\frac{D}{a}\right)^3 \quad (1)$$

$$N = \frac{M}{U} \quad (2)$$

All results were further verified by UV−vis spectrophotometry, where gold nanoparticles have a distinctive absorbance spectrum. Also, for all experiments the concentrations of the gold nanoparticles were equalized before incubation with cells.

In Figure 1, a plot of the number of gold nanoparticles in/on cells versus size of gold nanoparticles shows cellular uptake was heavily dependent upon the size. The maximum uptake by a cell occurred at a nanoparticle size of 50 nm. In agreement with our results, Osaki et al. qualitatively showed that 50 nm semiconductor nanoparticles entered cells via receptor-mediated endocytosis more efficiently than smaller nanoparticles. Figure 2 shows TEM images of gold nanoparticles with sizes between 14 and 100 nm inside cells and trapped in vesicles in the cytoplasm. They did not enter the nucleus. For a single cell, multiple vesicles containing gold nanoparticles are readily observed (see Supporting Information section 3). Within the vesicles, the nanoparticles appeared to be monodisperse (see Figure 2B-F). Figure 2A shows that the number of nanoparticles per vesicle diameter is related to the size of the gold nanoparticles. We used the unit of gold nanoparticles per vesicle size (area) because of vesicle size variations; this method allowed standardization of measurements. Further studies with gold nanoparticles coated with the specific ligand transferrin have a similar intracellular uptake trend as the citrate acid stabilized gold nanoparticle (see Supporting Information section 4). Transferrin is one of the many proteins in serum, and it enters cells via receptor-mediated endocytosis. However, the number of transferrin-coated gold nanoparticles entering the cells is ca. three times less than that of the citrate-stabilized gold nanoparticles. Finally, we conducted a trypan blue exclusion staining assay to determine cellular viability. Our results did not indicate any cellular toxicity due to uptake of gold nanoparticles (98% viability), which is in agreement with results by other research groups. [31−33]

Figure 3A shows the uptake of the nanoparticles significantly increased for the first 2 h, but the uptake rate gradually slowed and reached a plateau at 4− 7 h, depending on size. This plateau effect is in agreement with a previous study by Desai et al.[34] The uptake half-life determined by the slope of Figure 3a for the different-sized gold nanoparticles was 2.10, 1.90, and 2.24 h at a rate of 622, 1294, and 417 nanoparticles per hour for the 14, 50, and 74 nm gold nanoparticles, respectively. The maximum number of nanoparticles a cell can uptake for sizes 14, 50, and 74 nm are 3000, 6160, and 2988 respectively (see Figure 3B).

Initially, the mechanism of cellular uptake was puzzling since the overall surface charge of the gold nanoparticles

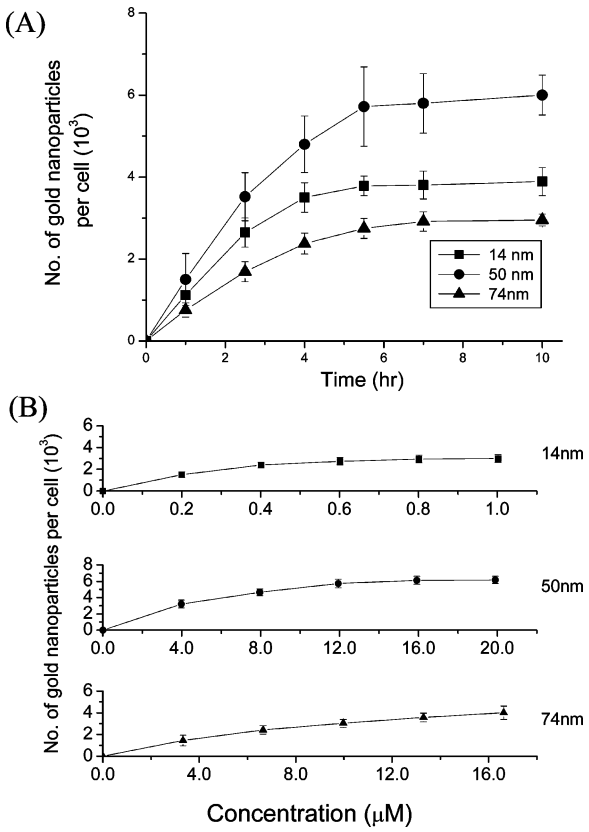

Figure 3. Cellular uptake kinetics of gold nanoparticles. (A) Cellular uptake of gold nanoparticles as a function of incubation time for three different size gold nanoparticles (nanoparticle diameters 14, 50, and 74 nm). (B) Dependence of cellular uptake of gold nanoparticles as a function of concentration (nanoparticle diameters 14, 50, and 74 nm).

was negative (due to the citric acid stabilizing ligand). Anionic molecules and structures bind less efficiently to cell surfaces than neutral or cationic molecules since electrostatic repulsion between the negatively charged surface membrane and cellular environment would repel the nanoparticles from entering. That is the reason why lysine-rich macromolecules and positively charged liposomes are commonly used for transfecting molecules into cells.[14]

We hypothesize the uptake of gold nanoparticles is mediated by nonspecific adsorption of serum proteins onto the gold surface; these proteins induce the nanoparticles to enter into cells via the mechanism of receptor-mediated endocytosis. To test out this hypothesis, we incubated gold nanoparticles with DMEM containing 10% serum, purified them by centrifugation (10 000 rpm), and analyzed them using UV−vis absorbance spectrophotometry, FTIR spectroscopy, gel electrophoresis, and protein assay (see Figure 4).

The absorbance spectra shows a shift in the surface plasmon resonance peak of 6 nm (Figure 4A) when the gold nanoparticles are incubated with DMEM plus 10% serum (marked in black in Figure 4A); previous studies show proteins adsorbed onto the gold nanostructures could cause similar shifts in the surface plasmon resonance.[35] The FTIR spectroscopy was used to verify the attachment of proteins on the surface of the gold nanoparticles. For gold nanopar-

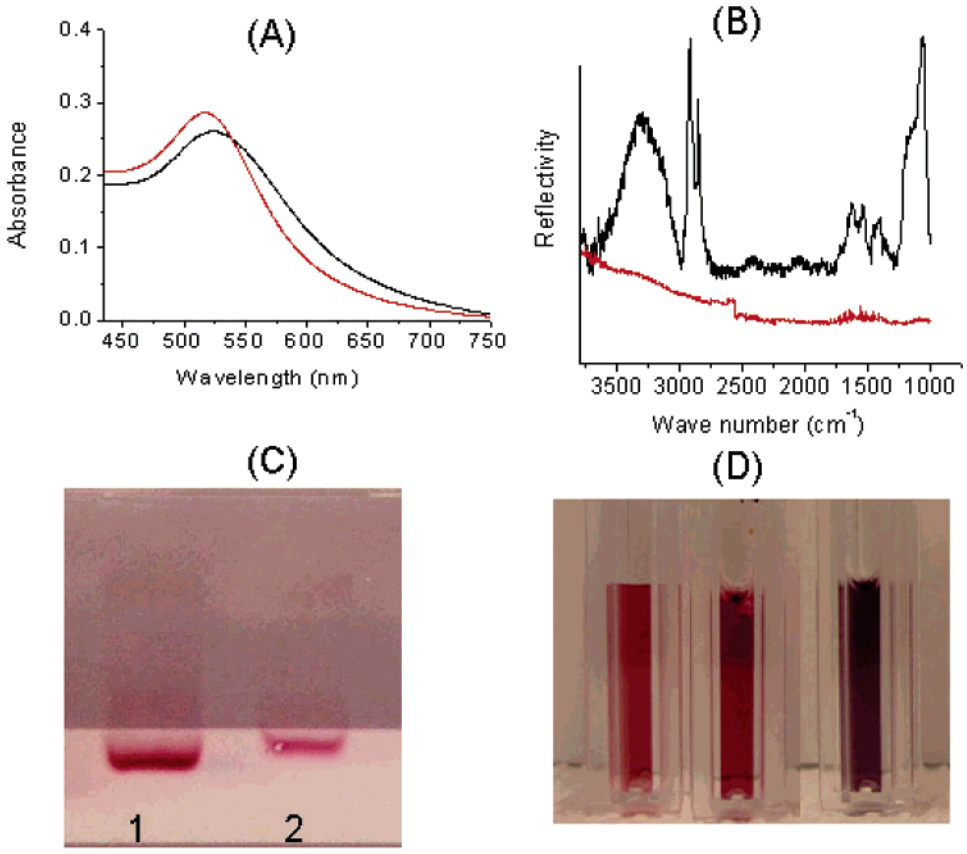

Figure 4. Determining the nonspecific adsorption of serum proteins on gold nanoparticles. (A) Absoption spectra of citrate-capped gold nanoparticles (marked in red) and gold nanoparticles capped with serum protein (marked in black). (B) FTIR spectra of serum protein capped gold nanoparticles (marked in black) in comparison to citrate-capped gold nanoparticles (marked in red). (C) Electrophoretic mobilty of citrate stabilized gold nanoparticles (lane 1) and serum protein stabilized gold nanoparticles (lane 2) in agarrose gel. Gel electrophoresis of citric acid stabilized gold nanoparticles in DMEM (without serum) was not studied due to aggregation of the gold nanoparticles in media. (D) Vials of citrate-capped gold nanoparticles (left most), serum protein capped gold nanoparticles (middle), and serum protein capped gold nanopaticles after incubation in a ninhydrin solution (right most). The purple color of the solution indicates the detection of primary and secondary amines (which are commonly in proteins). For brevity, we show data for the 50 nm gold nanoparticles. Similar results were found for other sizes and shapes.

ticles modified with serum protein, the peaks at 1550 and 1407 cm^{-1} indicate the presence of the primary amine on the nanoparticle surface. Broad band 3300 cm^{-1} is an indication of the bonded NH or NH_2 groups on the surface (see Figure 4B). The gel bands indicate loss of mobility (see lane 2 in Figure 4C) after incubation; alteration of nanoparticle surface charge or size can slow their mobility in a gel. Finally, a ninhydrin-based protein assay was conducted to verify that proteins are on the surface of gold nanoparticles. In the presence of high concentrations of primary and secondary amines (from amino acids), the solution becomes purple when incubated with the organic molecule ninhydrin after 10 min. Figure 4D shows vials of gold nanoparticles incubated in a ninhydrin solution after incubation in citrate buffer, DMEM, and DMEM plus serum followed by purification. Clearly, the vial of gold nanoparticles incubated with DMEM plus serum is purple. Of note, incubated gold nanoparticles with only DMEM lead to aggregation after 1 h. These data suggest that the surface of the gold nanoparticles was modified by nonspecific adsorption of serum proteins. This is likely since citric acid stabilizers are weakly bound to the surface of gold nanoparticles and could be desorbed from the metal surfaces by proteins. This adsorption process appears to be instantaneous.

As to the mechanism of entrance, our results show that the gold nanoparticles entered the cells via the receptor-mediated endocytosis pathway (RME). In RME, a ligand binds onto a receptor on the cell's surface and enters the cell when the membrane invaginates. Eventually, the receptor recycles back, meaning that it takes the ligand into the cell, releases the ligand, and then comes back onto the membrane surface. Cells have a maximum receptor density (number of receptors per cell surface area) on the membrane; the unbound or available receptors determine whether and how much a molecule or structure enters a cell via this mechanism. Since RME is dependent upon temperature, we compared the uptake of gold nanoparticles at 37 versus 4 °C. Our results show a vast difference in absorbance signal between cells incubated with gold nanoparticles at 37 versus 4 °C ($A_{560\ nm}$ per cell of 3×10^{-6} versus 1.54×10^{-6}, respectively). The background absorbance signal ($A_{560\ nm}$) for a cell is 1.22×10^{-6}. These results are in agreement with previous RME studies, where ligands did not enter cells at 4 °C but were only bound to the cell membrane.[36] We

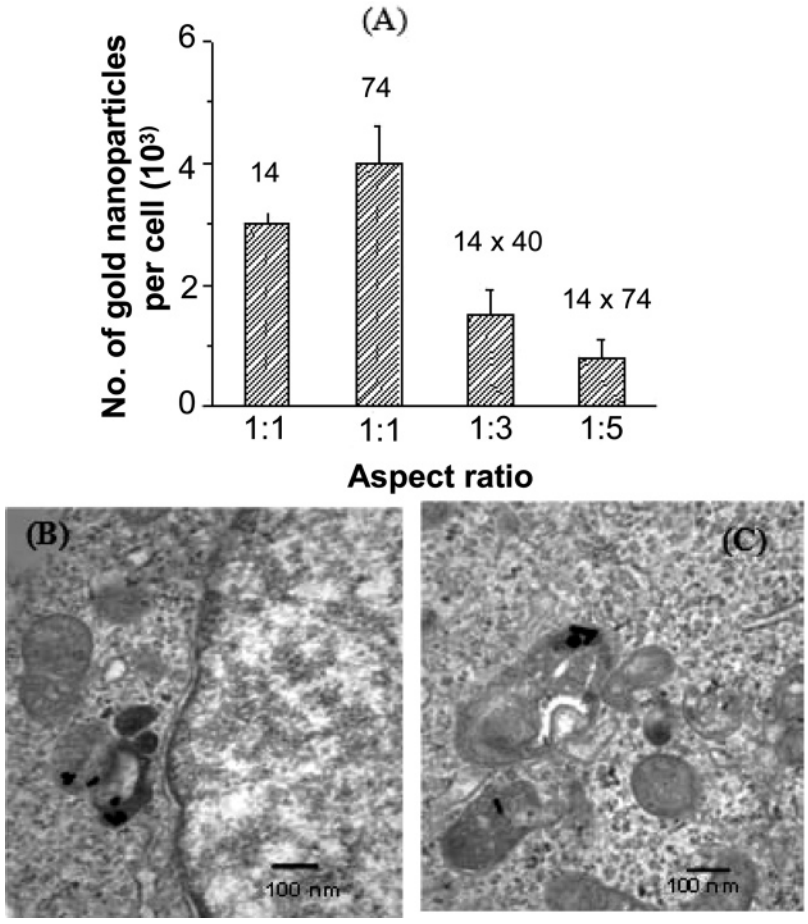

Figure 5. The effect of shape of the nanoparticles on cellular uptake and transmission electron microscopy images of rod-shaped gold nanoparticles internalized within the cells. (A) Comparison of uptake of rod-shaped nanoparticles (with aspect ration 1:3 and 1:5) and spherical shaped nanoparticles, the transmission electron microscopy images of rod-shaped gold nanoparticles with aspect ratio 1:3 (B) and 1:5 (C) internalized inside vesicles of Hela cells.

conclude that serum proteins are adsorbed on the nanoparticle surface and dictate the uptake of the nanoparticles.

To study the effect of nanoparticle shape on cellular uptake, we used spherical and rod-shaped gold nanoparticles. Figure 5A shows that nanoparticle uptake is dependent upon shape and that the uptake of rod-shaped gold nanoparticles is lower than their spherical counterpart. For example, cells took up 500 and 375% more 74 and 14 nm spherical gold nanoparticles than 74 × 14 nm rod-shaped gold nanoparticles, respectively. The difference in the surface chemistries (from the stabilizing ligand from the synthesis) between the spherical and rod-shaped gold nanoparticles may be one of the reasons for the difference in uptake. However, cellular uptake of rod-shaped structures with lower aspect ratio (1:3) is greater than higher aspect ratio (1:5) nanoparticles (both of these rod-shaped gold nanoparticles are synthesized in the presence of CTAB). In every TEM image, we observed a high population of nonrod-shaped nanoparticle byproducts in the cells along with rod-shaped nanoparticles (see Figure 5). Yet, spherical, cuboidal, and triangular-shaped gold nanoparticles constituted only 25% of the nanoparticle population after synthesis. We have included more images of rod-shaped nanoparticles taken up by the cells in the Supporting Information to show this low concentration in the vesicles was not an anomaly (see Supporting Information section 3). This suggests the actual number of rod-shaped gold nanoparticles entering cells is less than that depicted in Figure 5. ICP-AES does not discriminate the size and shape, and it is difficult to separate the different shaped nanoparticles before use in cell experiments. This result supports our claim that spherical-shaped particles have a higher probability of entering the cell in comparison to rod-shaped nanostructures.

On the basis of our results, we can speculate on the mechanisms that govern size- and shape-dependent intracellular uptake of nanoparticles. Clearly, nonspecific adsorption of serum proteins mediates the uptake of the nanoparticles. The presence of these proteins on the surface of the nanoparticles dictates uptake half-life, rates, and amount. A quantitative comparison of citrate-stabilized gold nanoparticles versus transferrin-coated nanoparticles clearly shows greater uptake of citrate-stabilzed gold nanoparticles. Since serum proteins contain a diverse set of proteins, the surface of the citrate-stabilized gold nanoparticles probably contains a variety of serum proteins on its surface. Many of the serum proteins (e.g, α- and β-globulin proteins) are known to be taken up by cells. Therefore, the diversity of the proteins may allow entrance into the cells via multiple receptors as compared to transferrin (which only has two corresponding receptors[37]). We want to note that the saturation rate of uptake

may also depend on the number of available proteins (that are not adsorbed onto the gold nanoparticles in the DMEM + serum) since these unbound proteins can compete for receptor sites on the cell surface against protein-adsorbed nanoparticles. Saturation curves, such as Figure 3, are commonly observed for receptor-mediated endocytosis. Since serum proteins are important in the internalization of gold nanoparticles, a further detailed study will be needed. This will provide a greater understanding of how citrate-stabilized gold nanoparticles enter the cell.

Even with the serum proteins dictating uptake, the size and shape of the nanoparticles appear to matter in the uptake scheme. We observed a large difference in the uptake of the different size and shaped gold nanoparticles. For example, the uptake concentrations for 74 × 14 nm rod-shaped nanoparticles were different than those for 74 or 14 nm spherical nanoparticles. At this point, we can only speculate as to the reasons. One reason could be the difference in the curvature of the different-shaped nanoparticles. For example, the rod-shaped nanoparticles can have larger contact area with the cell membrane receptors than the spherical nanoparticles when the longitudinal axis of the rods interacts with the receptors. This, in effect, could reduce the number of available receptor sites for binding. A second reason could be the amount of CTAB surfactant molecules adsorbed onto the rod-shaped nanoparticle surface during synthesis. If the CTAB was still on the surface, the serum protein may not be able to bind onto the gold nanoparticle surface efficiently. Also, the protein coating on the surface of the rod-shaped gold nanoparticles may not be homogeneous. In such a case, the ligands on the surface of the rod-shaped gold nanoparticles may not bind to receptors on the cell surface as strongly (due to a lack of multivalent binding). This would affect the uptake of the nanoparticles. More studies will be required. The results strongly suggest that nanoparticle size and shape can mediate receptor−ligand binding constants, receptor recycling rates, and exocytosis.

Many important applications of nanotechnology would not be achievable without the proper design of nanoparticles. As the integrative field of biomedical nanotechnology evolves, more systematic approaches for the chemical design of nanoparticles and structures will be required. Fundamental studies on the interface of nanostructures with biological systems will provide guidance. As researchers start to construct multifunctional nanostructures, issues of size and shape and surface chemistry will be important. In this study, we show that size and shape of the nanoparticles and nonspecific adsorption of proteins are important for maximal intracellular uptake. These results suggest that we can tune the delivery of proteins, drugs, and oligonucleotides using nanoparticles for diagnostic and therapeutic applications by the size and shape of the nanometer-scale structure. As to the broad issues of nanotoxicity, the nonspecific adsorption of serum protein(s) may dictate the cellular fate, uptake, metabolism, and clearance of nanoparticles. As new tools and probes emerge from nanotechnology research, such fundamental studies will be important.

Acknowledgment. W.C.W.C. would like to acknowledge CIHR, NSERC, CFI, OIT, and University of Toronto for financial support. D.B. and A.A.G. would like to thank NSERC and OGS for fellowships. We acknowledge Mrs. Tanya Hauck and Mr. Justin Chan for informative discussions on nanoparticle preparation and ICP-AES analysis. We acknowledge Mr. Battista Calvieri for his support in processing cells for transmission electron microscopy.

Supporting Information Available: The methods and experimental procedures and TEM images and absorption spectra of gold nanoparticles and TEM images of Hela cells with internalized nanoparticles. This material is available free of charge via the Internet at http://pubs.acs.org.

References

(1) El-Sayed, I. H.; Huang, X.; El-Sayed, M. A. *Nano Lett.* **2005**, *5*, 829−834.
(2) Veiseh, O.; Sun, C.; Gunn, J.; Kohler, N.; Gabikian, P.; Lee, D.; Bhattarai, N.; Ellenbogen, R.; Sze, R.; Hallahan, A.; Olson, J.; Zhang, M. *Nano Lett.* **2005**, *5*, 1003−1008.
(3) Parak, W. J.; Boudreau, R.; Gros, M. L.; Gerion, D.; Zanchet, D.; Micheel, C. M.; Williams, S. C.; Alivisatos, P. A.; Larabell, C. A. *Adv. Mater.* **2002**, *14*, 882−885.
(4) Chan, W. C. W.; Nie, S. M. *Science* **1998**, *281*, 2016−2018.
(5) Bruchez, M.; Moronne, M.; Gin, P.; Weiss, S.; Alivisatos, A. P. *Science* **1998**, *281*, 2013−2016.
(6) Jiang, W.; Papa, E.; Fischer, H.; Mardyani, S.; Chan, W. C. W. *Trends Biotechnol.* **2004**, *22*, 607−608.
(7) Karhanek, M.; Kemp, J. T.; Pourmand, N.; Davis, R. W.; Webb, C. D. *Nano Lett.* **2005**, *5*, 403−407.
(8) Taton, T. A.; Lu, G.; Mirkin, C. A. *J. Am. Chem. Soc.* **2001**, *123*, 5164−4165.
(9) Medintz, I.; Clapp, A. R.; Melinger, J. S.; Deschamps, J. R.; Mattoussi, H. *Adv. Mater.* **2005**, *17*, 2450−2455.
(10) Panyam, J.; Labhasetwar, V. *Adv. Drug Delivery Rev.* **2003**, *5*, 329−347.
(11) Yang, P.; Sun, X.; Chiu, J.; Sun, H.; He, Q. *Bioconjugate Chem.* **2005**, *16*, 494−496.
(12) Kohler, N.; Sun, C.; Wang, J.; Zhang, M. *Langmuir* **2005**, *21*, 8858−8864.
(13) Chenevier, P.; Veyret, B., Roux, D.; Henry-Toulme, N. *Biophys. J.* **2000**, *79*, 1298−309.
(14) Lee, K.-D.; Nir, S.; Papahadjopoulos, D. *Biochemistry* **1993**, *32*, 889−99.
(15) Miller, C. R.; Bondurant, B.; McLean, S. D.; McGovern, K. A.; O'Brien, D. F. *Biochemistry* **1998**, *37*, 12875−12883.
(16) Carmona-Ribeiro, A. M.; Ortis, F.; Schumacher, R. I.; Armelin, M. C. *Langmuir* **1997**, *13*, 2215−18.
(17) Alyaudtin, R. N.; Reichel, A.; Lobenberg, R.; Ramge, P.; Kreuter, J.; Begley, D. J. *J. Drug Targeting* **2001**, *9*, 209−221.
(18) Jaulin, N.; Appel, M.; Passirani, C.; Barratt, G.; Labarre, D. *J. Drug Targeting* **2000**, *8*, 165−72.
(19) Shukla, S.; Priscilla, A.; Banerjee, M.; Bonde, R. R.; Ghatak, J.; Satyam, P. V.; Sastry, M. *Chem. Mater.* **2005**, *17*, 5000−5005.
(20) Chen, J.; Saeki, F.; Wiley: B. J.; Cang, H.; Cobb, M. J.; Li, Z.-Y.; Au, l.; Zhang, H.; Kimmey, M. B., Li, X.; Xia, Y. *Nano Lett.* **2005**, *5*, 473−477.
(21) Yang, P.-H.; Sun, X.; Chiu, J.-F.; Sun, H.; He, Q.-Y. *Bioconjugate Chem.* **2005**, *116*, 494−496.
(22) Hirsch, L. R.; Stafford, R. J.; Bankson, J. A.; Sershen, S. R.; Rivera, B.; Price, R. E.; Hazle, J. D.; Halas, N. J.; West, J. L. *Proc. Natl. Acad. Sci. U.S.A.* **2003**, *100*, 1549−1554.
(23) Loo, C.; Lin, A.; Hirsch, L.; Lee, M. H.; Barton, J.; Halas, N.; West, J.; Drezek, R. *Technol. Cancer Res. Treat.* **2004**, *3*, 33−40.
(24) Chen, J.; Wiley: B.; Campbell, D.; Saeki, F.; Cang, L.; Au, L.; Lee, J.; Li, X.; Xia, Y. *Adv. Mater.* **2005**, 17, 2255.
(25) Hainfeld, J. F.; Slatkin, D. N.; Smilowitz, H. M. *Phys. Med. Biol.* **2004**, *49*, N309−N315.
(26) Frens, G. *Nat. Phys. Sci.* **1973**, *241*, 20−23.

(27) Freeman, R. G.; Grabar, K. C.; Allison, K. J.; Bright, R. M.; Davis, J. A.; Guthrie, A. P.; Hommer, M. B.; Jackson, M. A.; Smith, P. C.; Walter, D. G.; Natan, M. J. *Science* **1995**, *267*, 1629−1632.
(28) Nikoobakht, B.; El-Sayed, M. *Langmuir* **2003**, *15*, 1957−1962.
(29) Sau, T. P.; Murphy, C. J. *Langmuir* **2004**, *20*, 6414−6420.
(30) Osaki, F.; Kanamori, T.; Sando, S.; Sera, T.; Aoyana, Y. *J. Am. Chem. Soc.* **2004**, *126*, 6520−6521.
(31) Connor, E. E.; Mwamuka, J.; Gole, A.; Murphy, C. J.; Wyatt, M. D. *Small* **2005**, *1*, 325−327.
(32) Uhlson, C.; Harrison, k.; Allen, C. B.; Ahmad, S.; White, C. W.; Murphy, R. C. *Chem. Res. Toxicol.* **2002**, *15*, 896−906.
(33) Goodman, C. M.; McCusker, C. D.; Yilmaz, T.; Rotello, V. M. *Bioconjugate Chem.* **2004**, *15*, 897−900.
(34) Desai, M. P.; Labhasetwar, V.; Walter, E.; Levy, R. J.; Amidon, G. L. *Pharm. Res.* **1997**, *14*, 1568−1578.
(35) Joshi, H.; Shirude, P. S.; Bansal, V.; Ganesh, K. N.; Sastry, M. *J. Phys. Chem. B* **2004**, *108*, 11535−11540.
(36) Foerg, C.; Ziegler, U.; Fermandez-Carneado, J.; Giralt, E.; Rennert, R.; Beck-Sickinger, A. G.; Merkle, H. P. *Biochemistry* **2005**, *44*, 72−81.
(37) Qing, X. M.; Li, H.; Sun, H.; Ho, K. *Pharmacol. Rev.* **2002**, *54*, 561−587.

NL052396O